MET.O.11 TECHNICAL NOTE No. 57

A Representation of topography and the Surface Boundary layer in the Meteorological Office 10-level Model

by F. R. Hayes

Summary

The current formulation of the friction layer and the treatment of topography are described. In contrast, a formulation is presented in which the friction layer is modelled at the topographic height, rather than at 1000mb, and the horizontal components of velocity are set to zero below this height. Results of experiments are shown for both the Rectangle and Octagon versions of the 10-level model, with reference in particular to a case in which the Octagon operational version produced a spurious high of 1100mb over the Himalayas. This problem was eliminated using the new formulation.

Introduction

A description of the Bushby-Timpson 10-level model on a fine mesh is given by Benwell et. al. (1971). The model is used by the Meteorological Office in two versions; a Northern Hemisphere 'Octagon' version, and a fine mesh North Atlantic 'Rectangle' version. The treatment of topography and friction is similar in both versions.

Friction is modelled by assuming a friction layer between the lowest two levels in the model, viz 1000 and 900mb. Frictional forces enter into the equation of motion as a term: $g\frac{\partial \underline{\tau}}{\partial p}$. In the paper, the term is calculated as $g\underline{\tau}_{1000}/100$ at 1000mb, and $g\underline{\tau}_{1000}/200$ at 900mb. However, later versions of the model compute $g\frac{\partial \underline{\tau}}{\partial p}$ at 1000mb as $g\underline{\tau}_{1000}/50$, and 0 at 900mb, since $\underline{\tau}$ does not vary linearly with pressure through the boundary layer, and a better approximation to $g\frac{\partial \underline{\tau}}{\partial p}$ at the surface is the latter (see Fig.1)

$\underline{\tau}$ is derived from the expression:

$$\underline{\tau} = -\rho_{1000} C_D |\underline{v}_{1000}| \underline{v}_{1000}$$

The value of C_D is given by:

$$C_D = \left(1.0 + \frac{H}{400}\right) \times 10^{-3} \quad \text{over land}$$

$$C_D = 0.7 \times 10^{-3} \quad \text{over sea}$$

where H is the smoothed topographic height. The variation of C_D over land is to prevent large discontinuities at the coast lines, and also to model a form drag over regions of high topography.

A criticism of this formulation of the surface boundary layer is that over areas of high topography, the drag coefficient takes on very large values. For instance, over the Himilayas, it reaches 13.2×10^{-3}, and over Greenland, a value of 9.0×10^{-3} is exceeded, compared to a sea-level value of 1.0×10^{-3}. Furthermore, the friction term is always applied at 1000mb, even when the topography extends much higher into the atmosphere. Greenland goes up to 700mb, and the Himalayas reach 550mb.

Topography is included in two aspects of the model, one of which is the

variation of Drag coefficient described above, the other being the representation of the lower boundary condition, the 'tendency' equation. The condition simply states that no fluid particles may cross the surface of the earth. In mathematical form, this becomes,

$$w = \underline{v} \cdot \nabla_H H$$

where $\underline{v}$ is the horizontal velocity, (u,v)

This equation is applied at 1000mb at each grid point.

Friction Layer in the Fluid

In order to represent more realistically the effects of the surface boundary layer, it is proposed to apply the friction term in the equations of motion at the topographic height, rather than at 1000mb. The stress vector is taken as:

$$\underline{\tau} = -\rho C_D |\underline{v}| \underline{v}$$

the value being computed from variables at the level next above topography. In a similar way to the present formulation, a surface boundary layer 50mb thick is assumed, and $g\frac{\partial \tau}{\partial p}$ is calculated as $g\tau/50$. Since the topography height lies between two levels, only a part of the friction layer affects the level above topography, and the friction term is multiplied by a fraction α to allow for this. α is defined in Fig.2 by:

$$\alpha = \frac{H - h_2}{h_1 - h_2}$$

The level next below topography may also be affected by the friction layer. The value of a variable at a level may be thought of as representing the mean value of a 100mb thick layer centred on that level. If any part of that 100mb layer is above the level of topography ($\alpha < 0.5$), a new friction term is computed for the lower level using the velocity from that level, and is added to the equation of motion, but without multiplication by α . Thus if $\alpha < 0.5$, the effective result is to model a friction layer for the level immediately below topography as well. If $\alpha \geq 0.5$, the layer represented by the level is completely below the ground. This case is dealt with in the next section.

In this version, the drag coefficient C_D is chosen not to vary with topographic height, and a constant value of 2.0×10^{-3} is used over land. Over sea, the representation remains unchanged.

The velocity below the topographic height

By modelling the friction layer at the topographic height in the model, there is an implied assumption that the fluid modelled below this height is ficticious. Neverthless, the technical problems of simply dropping several levels in the model where high topography exists are considerable, and it is simpler to allow air to exist below topography and attempt to prevent spurious circulations being set up 'underground'. There are various possibilities; one is to model a boundary layer in place of the topography, i.e. apply $g\frac{\partial \tau}{\partial p}$ at levels below the topography. However, this does not completely remove all spurious circulations, and some large divergences may be formed below the topography. The simplest, and physically most realistic solution is to have a 'no flow' condition below the ground, and allow this air to statically adjust itself to conditions at the surface of the earth. This condition is

approximately achieved by setting $u = v = 0$ under the ground. In this case, $\partial\omega/\partial p$ is zero under the ground, and ω is thus constant with pressure below the surface of the earth, and is equal to the surface value. Also, the tendency equation reduces to $w = 0$ at 1000mb, so there is no vertical motion across the lowest level of the model. Thus at 1000mb, the 'no flow' condition is exact. At levels above 1000mb, fluid particles below the topographic height are constrained to move only vertically.

The governing equations in operation below the topographic height became:

$$u = v = 0$$

$$\frac{\partial \omega}{\partial p} = 0$$

$$\frac{\partial h'}{\partial t} + \omega \frac{\partial h'}{\partial p} + \omega h' \left(\frac{1-K}{p}\right) = K \nabla^2 h'$$

$$\frac{\partial \tau}{\partial t} + \omega \frac{\partial \tau}{\partial p} = K \nabla^2 \tau$$

$$\frac{\partial h_{1000}}{\partial t} + \omega \frac{\partial h_{1000}}{\partial p} = K \nabla^2 h_{1000}$$

It would be most desirable to have the condition:

$$w = \underline{v} \cdot \nabla_u H$$

satisfied at the level of topography. In the new formulation, this condition is approximately satisfied when the topography lies below the 950mb level as in the current formulation. However, when the topography extends above this level, the boundary condition reduces to $w = 0$ at 1000mb, and the effects of topographic slope are induced in the areas of divergence or convergence at the boundary between the ground and the free atmosphere in the model. There is some loss in accuracy since the process of setting $u = v = 0$ is effectively constraining the topography to lie on one or other of the model levels. However, the experimental evidence indicates that the advantages of placing physical barriers in the model outweigh this possible loss of accuracy.

Results

The new formulation was tested for both Octagon and Rectangle versions of the 10-level model, for a variety of dates, including the 12 - 16 April 1974, when the Octagon version of the new formulation was run in parallel with the operational version for a total of 5 forecasts. Also various other dates were chosen, in particular the forecast from 12Z 20 February 1974 in which the operational octagon version produced spurious anticyclogenesis over the Himilayas. Other cases were chosen to demonstrate the effect of the new formulation when the operational version produced unrealistic gradients of pressure over high topography, poor cyclogenesis near regions of high topography and overdevelopment of certain systems. The cases were mostly from the winter months, since cyclonic activity was greatest, but a summer case was chosen for completeness, to illustrate the effect when the level of cyclonic activity was low.

In addition a series of Rectangle version forecasts has been run, to illustrate the effect of the new formulation in cases similar to those outlined above.

Results from Octagon version - surface pressure forecasts

A. Parallel Run 12 - 16 April.

Forecasts were run on midnight data for 5 consecutive days from 12 - 16 April 1974, in parallel with the operational forecasts. On the whole, the forecasts were quite similar, but with a few exceptions. Differences in central pressures of cyclones were of the order of 1 - 2mb, with no clear trend indicating whether the new formulation was better or worse than the current operational forecast. Centres of high pressure were generally similar, but the shapes of high cells were sometimes different, notably over the U.K. Some of the forecasts (see Figs. 6 - 8) were very poor over the Atlantic area. However, both versions were very similar in this case, that is, both forecasts were inaccurate.

Figures 3 - 5 show the results of the forecast based on 00Z 16.4.72 data for T + 72. The most noteworthy feature in the forecasts is a low of 1006mb centred over the Black Sea. The operational forecast had deepened this low too much, and at T + 72 the central pressure was 986mb, too deep by 20mb. The new formulation, however, deepened the low to 994mb; too deep, but this time by 12mb. Both versions handled the low inaccurately, but the new formulation was closer by 8mb to the analysed central value.

Figures 6 - 8 show the results of the forecast based on 00Z 14.4.74 data, for T + 48. The poor forecast over the Atlantic is noticeable, the new formulation performing only marginally better.

B. Forecast data time 12Z 20 February 1974

The main reason for testing this forecast was a response to a pressure pattern suggesting some weak instability close to high topography in the operational version. Over a period of several days, a spurious high was built during the forecasts in the region of the Himalayas. The Laplacian of pressure in this area became very large, thus producing a diffusion term large enough to remove the spurious high pressure by T + 72. In the forecast indicated in Fig.9, that from data at 12Z 20 February 1974, the high pressure cell had built to greater than 1100mb. Winds at 1000mb were small, but at 900mb, there were large values of divergence in this area.

Figure 10 shows the new formulation version of this forecast. The instability is completely absent. Figure 11 is the corresponding analysis for this forecast.

C. Other Forecasts

Figures 12 - 14 show the forecast based on 12Z 14 March 1974 data, for T + 48 together with the corresponding analysis. Again the operational version is suggesting some weak instability over the Himalayas, which is completely removed in the new formulation. In addition, there is a rather tight gradient of pressure over Greenland in the operational version. This is a fairly common feature of current winter forecasts. The tight gradient is caused by the building of a high cell on the Eastern coast of Greenland. The new formulation moved the high pressure centre further eastwards, reducing its intensity somewhat,

and produced much smoother gradients of pressure over the Greenland massiff.

Figures 15 - 17 illustrate a case of cyclogenesis near the southern tip of Greenland. The forecasts are from 12Z 23 December 1973 data. A low from the Newfoundland area moved north, up the western coast of Greenland. The low did not split, but a new low was formed just southeast of the tip of Greenland, and it moved north-eastwards. At 12Z on the 24th, the new low had a central pressure of 975mb according to CFO charts. The analysis in Fig.17 does not show the low, possibly dus to sparse data and a poor background field. This chart has a pressure of 982mb at the true position of the low. The operational forecast did not produce low centre, but a marked trough, with a pressure of 994mb at the true position of the low. The new formulation had a low centre, with a central pressure of 990mb, in the correct position. At later stages in the forecast, the new formulation moved this low correctly, whereas the operational version finally produced a shallow depression from the trough and also another spurious centre on the tip of Greenland. The pressure pattern in this area became rather confused. The parent low was handled better by the operational version having its central pressure forecast 5mb not deep enough, with the new formulation in error by 10mb. The corresponding initialisation is itself in error by 7mb, presumably for the reasons cited above.

For completeness, a summer case was chosen at random to indicate the effect on situations with low cyclonic activity. Figs. 18 and 19 are the forecasts for 00Z 15 August 1973 data at T + 24. As might be expected, the lower mean wind speeds were less affected by friction, and the two forecasts are similar, the differences being practically insignificant.

Results from the Rectangle Version - surface pressure forecasts.

Forecasts run on the Rectangle version of the new formulation reflected similar characteristics found in the octagon version, particularly in the development or decay of cyclones in regions of high topography.

Figures 20 - 22 are the analysis, and the two 36 hour forecasts verifying at 12Z 3.4.73. An intense depression had moved rapidly over the UK during the forecast, deepening as it crossed the North Sea. On encountering land, it slowly filled. At the time shown it was over the Baltic Sea, with a central pressure of 994mb. Both versions forecast the position of the low at this time, although the operational version gave a central pressure of 983mb. The new formulation was 990mb, closer by 7mb. A trough associated with this low crossed the Alps during the forecast period, forming into a shallow low centre over Northern Italy. Neither version produced a low centre, but the new formulation did produce a realistic ridging over the Alps, present in the analysis, but absent in the operational version, and also a drop of 3mb pressure from the operational version in the North Italy region. In addition, the new formulation gave greater rainfall rates in the trough, producing an unbroken line of frontal rain back to the parent depression. The gradient of pressure over Greenland was also less intense in the new version, although the old depression on the south eastern coast of Greenland had been incorrectly filled by 1-2mb.

Figures 23 - 25 represent the analysis together with forecasts verifying at 00Z 6.4.73. During the forecast, a depression off the south coast of Greenland moved eastwards. In its place a ridge was extended southwards so that at 00Z on the 6th, pressure was built to 1026mb at the tip of Greenland. The operational version, rather than building the ridge, proceeded to form a second depression in this area, without rise of pressure, so that, at T + 36,

a spurious low was forecast with a central pressure of 991mb, in error by 35mb. The new formulation did not predict the formulation of a second low, but built pressure in the area, although not sufficient to extend the ridge into the area by the end of the forecast period. At this time, the pressure was in error by 18mb in this area, an improvement of 17mb compared to the operational, although the pressure pattern was still forecast incorrectly as a trough, rather than a ridge.

Figures 26 - 28 illustrate a further example of excessive pressure gradients over Greenland, and also incorrect deepening of a low in the operational forecast. The verification time for the charts is 12Z 30.11.73. The new version is seen here to prevent the building of high pressure on the eastern side of Greenland, thus reducing the intense gradient of pressure found in the operational version.

A depression over France at T+0, moved eastwards, splitting into 2 centres. One centre continued eastwards, and left the forecast area, whilst the other moved approximately south eastwards, ending up over Greece at T+36 with a central pressure 1002mb. Both versions of the forecasts failed to split the depression and the operational version deepened it to 986mb, and moved it much too slowly, so that at T+36 it was misplaced by about 700km. The new version did not deepen the low so much and moved it slightly faster, so that at T+36, the central pressure was 994mb, and 100km further on. Some roughnesses were apparent in the region of this low in the new formulation.

300mb winds and mean statistics

During the series of parallel run forecasts, mean statistics were compiled for the octagon area, and also charts of 300mb winds output. Change in the new formulation forecast winds were generally very small. In a few instances, the jet maximum wind speed was increased, but this was balanced by instances of the jet maximum wind speed decreasing. In the forecast based on 00Z 15.4.74 data, at T+24, a jet was decreased from 123kt to 121kt at the maximum. In the forecast based on 00Z 16.4.74 at T+24, another jet was increased from 119kt to 120kt.

The mean statistics indicated that with the new formulation there was a drop in the 300mb mean square wind speeds of about 2%. In addition the mean total rainfall accumulations fell by 2%, although it was generally observed in the forecasts that locally the new formulation could have a beneficial effect on rainfall totals.

Conclusions

The new version, incorporating the friction layer modelled at the topographic height, and $\underline{v}$ set to zero below the topography, has been tested with 12 Octagon forecasts and 8 Rectangle forecasts, a selection of which have been presented in the previous section. In no case did the new formulation produce a forecast which was seriously worse than the corresponding operational forecast, although the central pressures of a few lows were more in error than the operational forecast by 2-4mb.

The new formulation has shown that it has significantly improved forecasts, particularly in the cases of: cyclogenesis, cyclone decay, prevention of spurious cyclogenesis and rainfall patterns in the region of high topography. In addition, it has prevented the formation of unrealistic pressure patterns over high topography, especially over Greenland, and in the extreme case of the Himalayas. Over the Alps it produced a realistic ridge-trough associated

with the high ground. These improvements have been observed in both the rectangle and octagon versions of the new formulation.

References

Benwell, G.R.R., Gadd, A.J., Keers, J.F., Timpson, M.S., and White, P.W. - "The Bushby-Timpson 10-level Model on a Fine Mesh". Met.Office Sci.Paper No.32 (1971) HMSO.

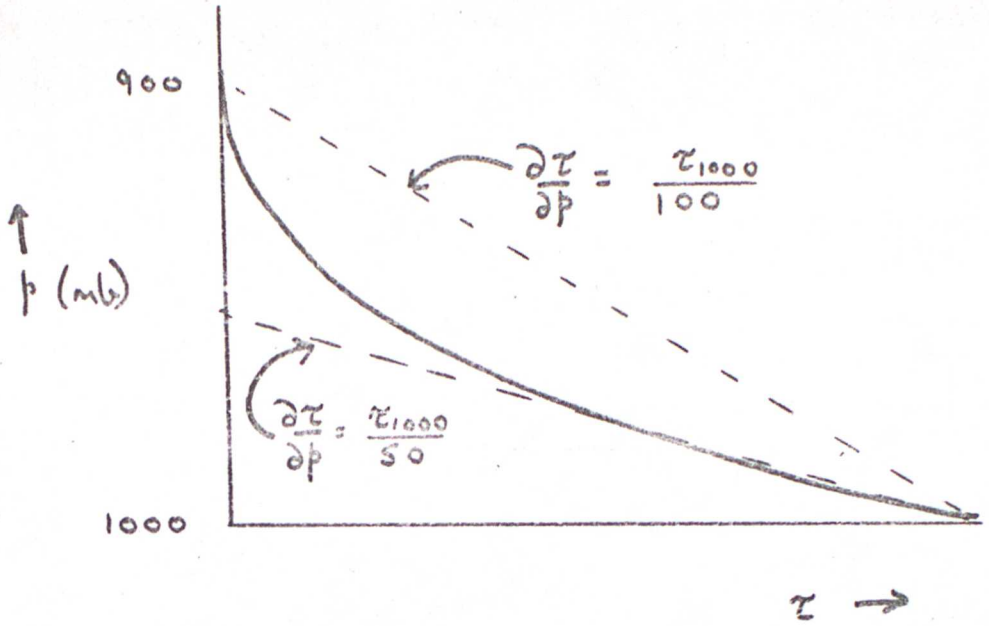

FIG. 1 FINITE-DIFFERENCE REPRESENTATIONS OF $\frac{\partial \tau}{\partial p}$

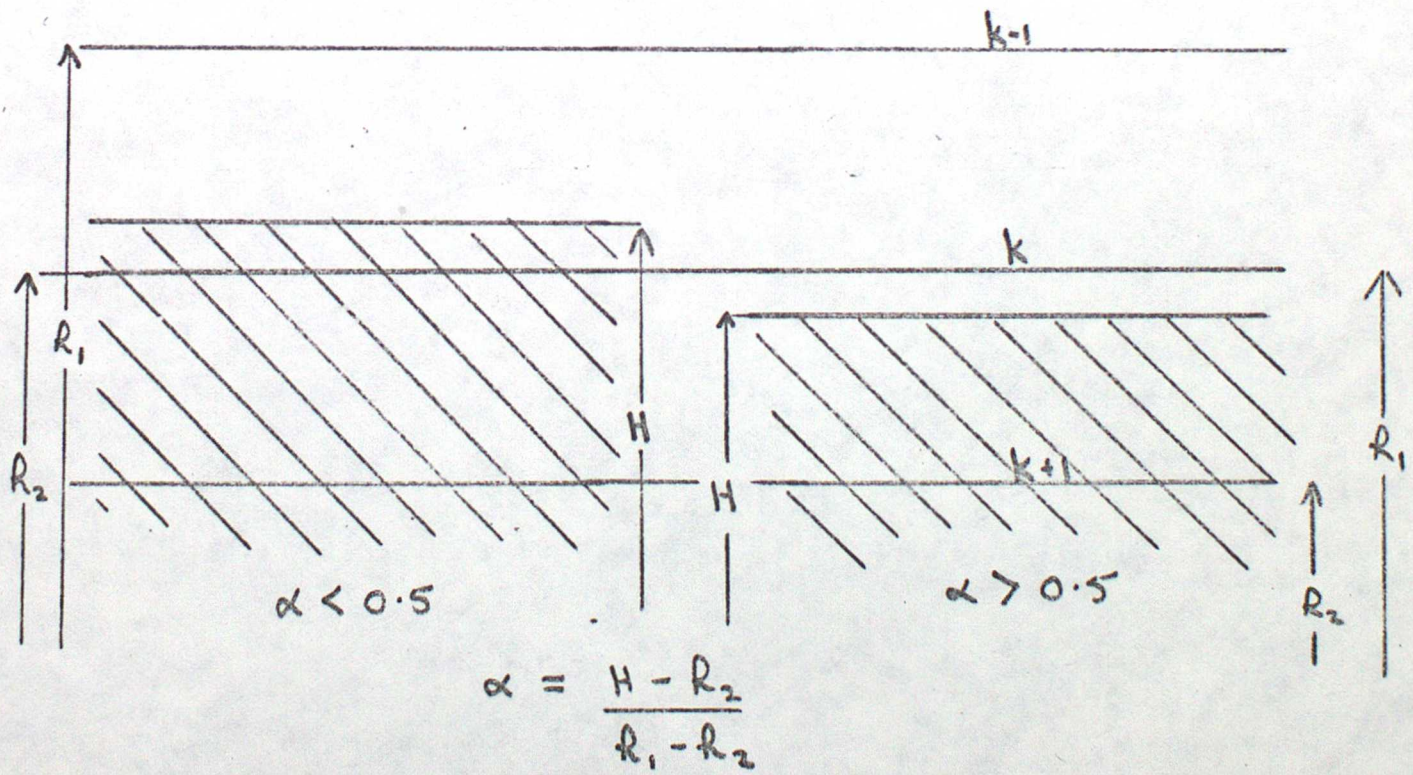

FIG 2 POSSIBLE POSITIONS OF TOPOGRAPHY RELATIVE TO MODEL LEVELS

FIG. 3

OPERATIONAL F/C

T+72

VERIFYING: 00Z 19/4/74

FIG. 4

NEW

FORMULATION F/C

T+72

VERIFYING: 00Z 19/4/74

FIG. 5

ANALYSIS

00Z 19/4/74

FIG. 6

ANALYSIS

00Z 16/4/74

FIG. 7

OPERATIONAL F/C

T + 48

VERIFYING: 00Z 16/4/74

FIG. 8

NEW

FORMULATION F/C

T + 48

VERIFYING: 00Z 16/4/74

FIG. 9

OPERATIONAL F/C

T+48

VERIFYING: 12Z 22/2/74

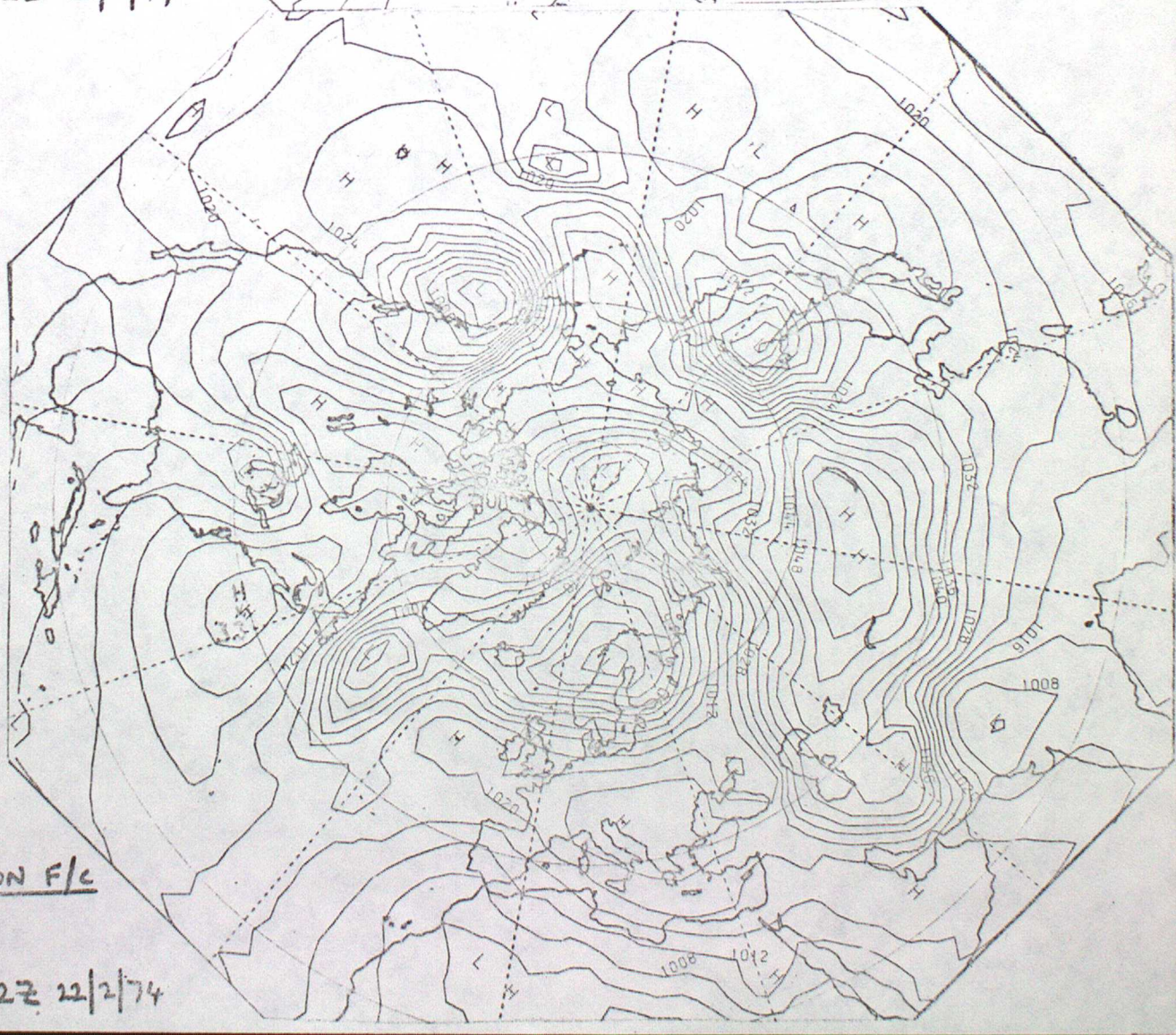

FIG. 10

NEW

FORMULATION F/C

T+48

VERIFYING: 12Z 22/2/74

FIG. 11

ANALYSIS

12Z 22/2/74

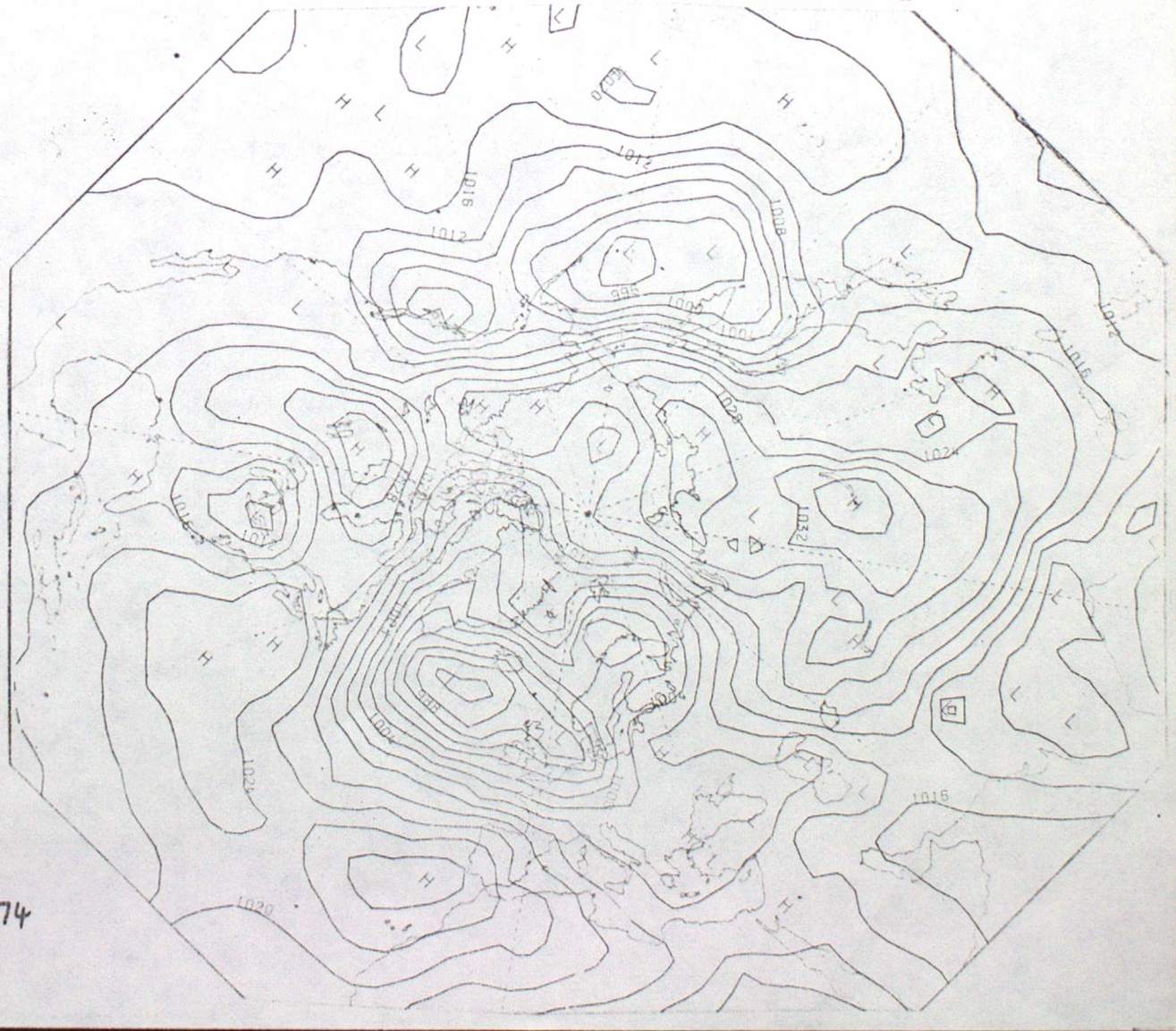

FIG. 12

ANALYSIS

12Z 16/3/74

FIG. 13

OPERATIONAL F/C

T+48

VERIFYING: 12Z 16/3/74

FIG. 14

NEW

FORMULATION F/C

T+48

VERIFYING: 12Z 16/3/74

FIG. 15

OPERATIONAL F/C

T+24

VERIFYING: 12Z 24/12/73

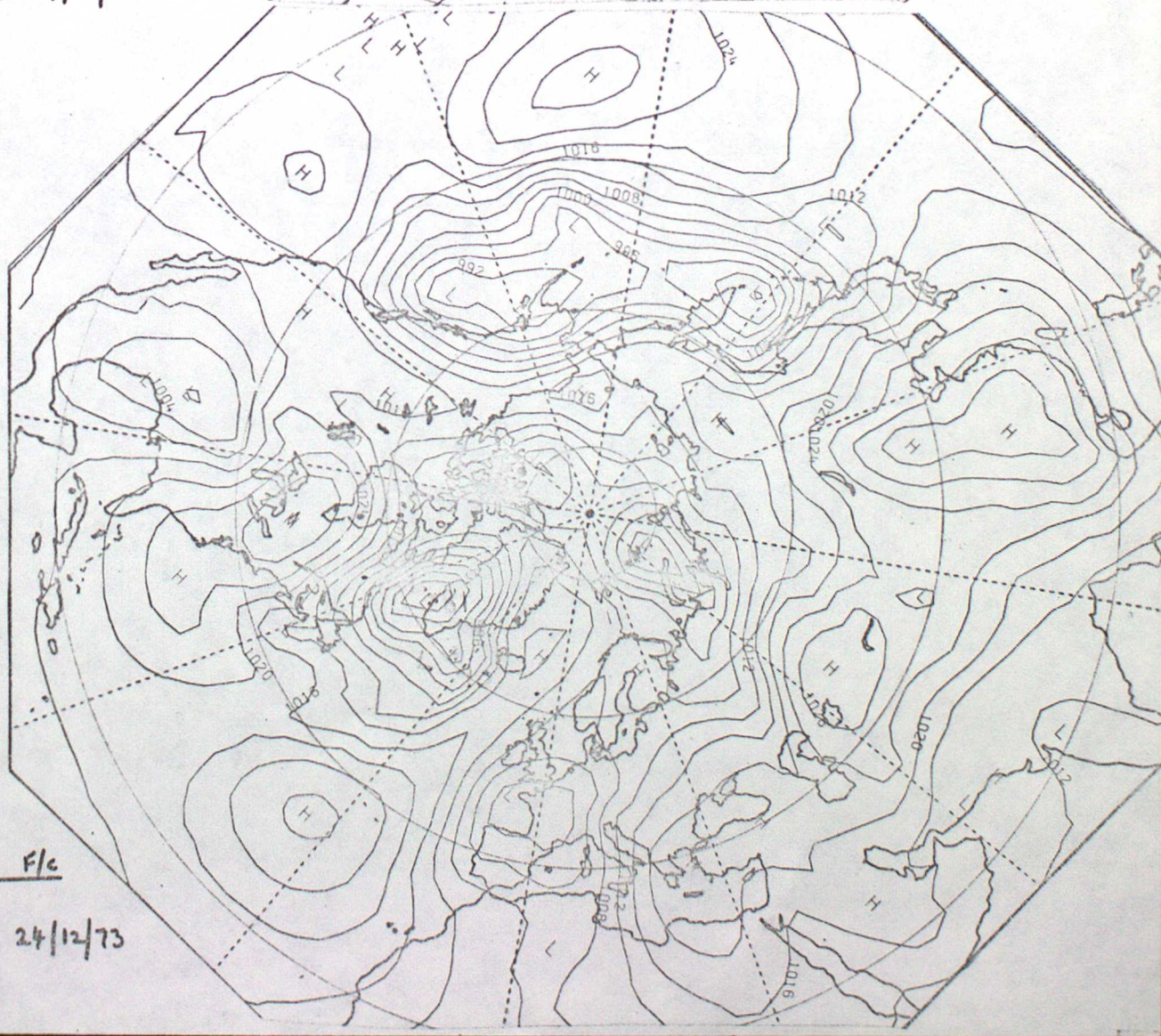

FIG. 16

NEW

FORMULATION F/C

T+24

VERIFYING: 12Z 24/12/73

FIG. 17

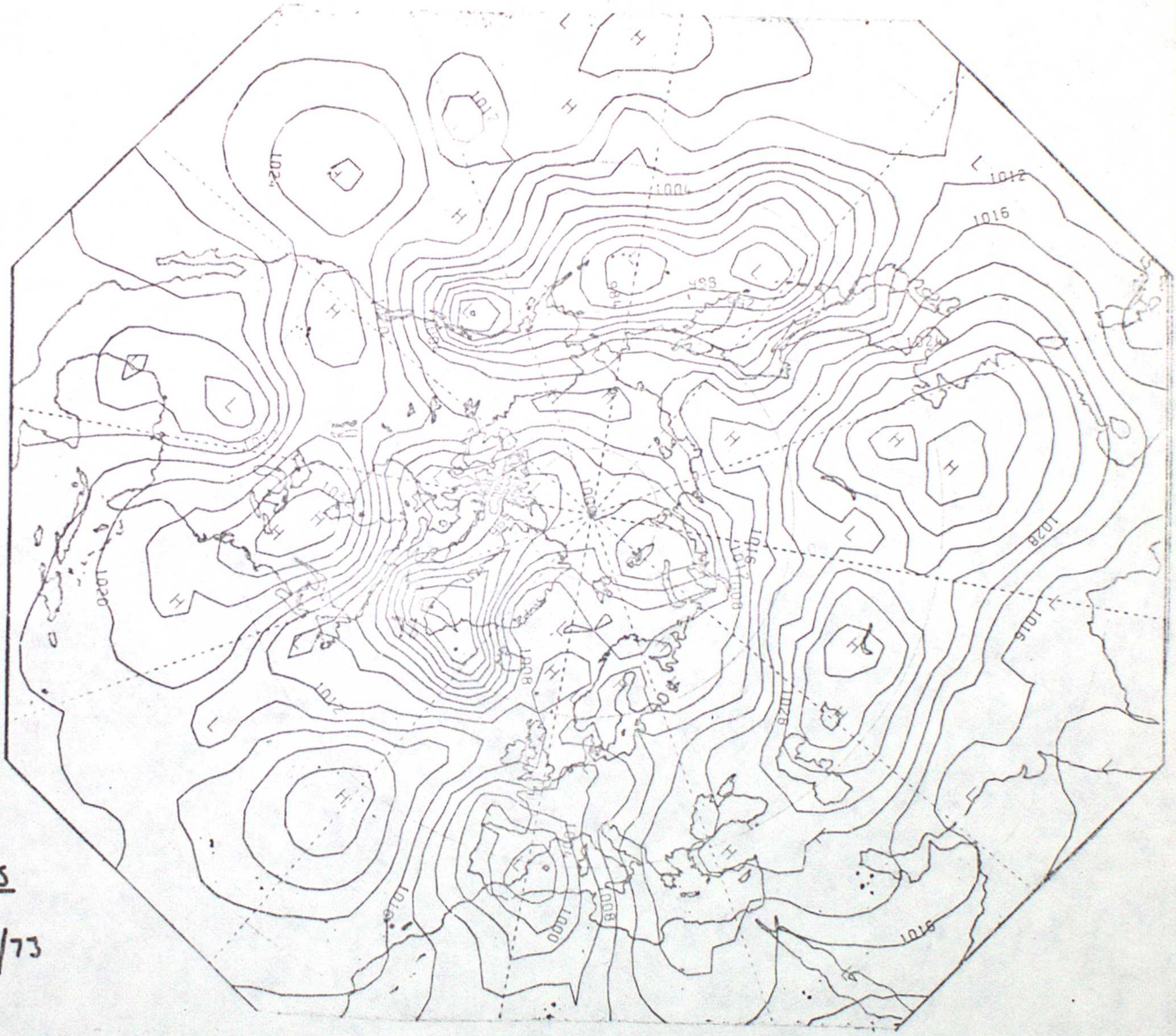

ANALYSIS

12Z 24/12/73

FIG. 18

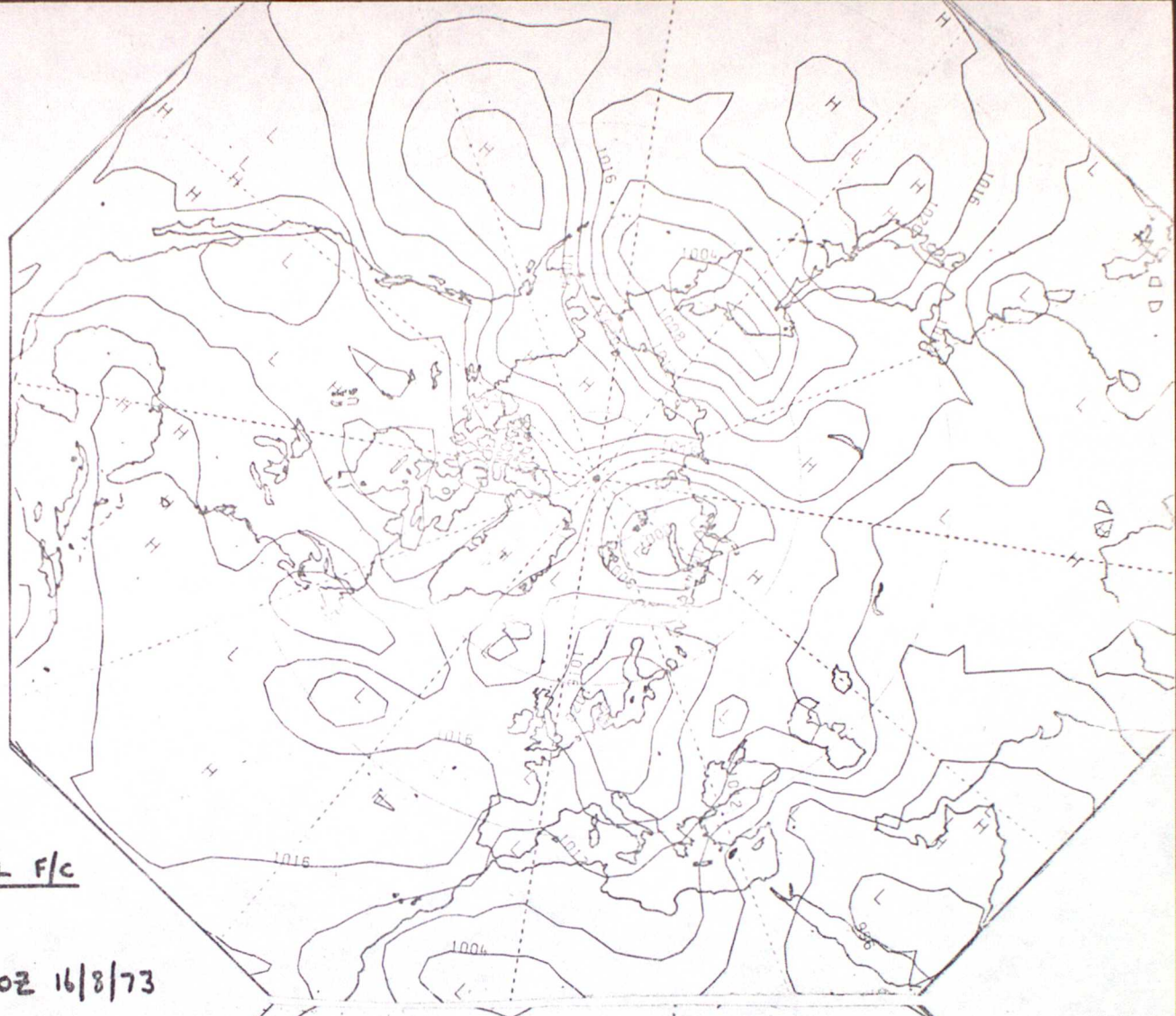

OPERATIONAL F/C

T + 24

VERIFYING: 00Z 16/8/73

FIG. 19

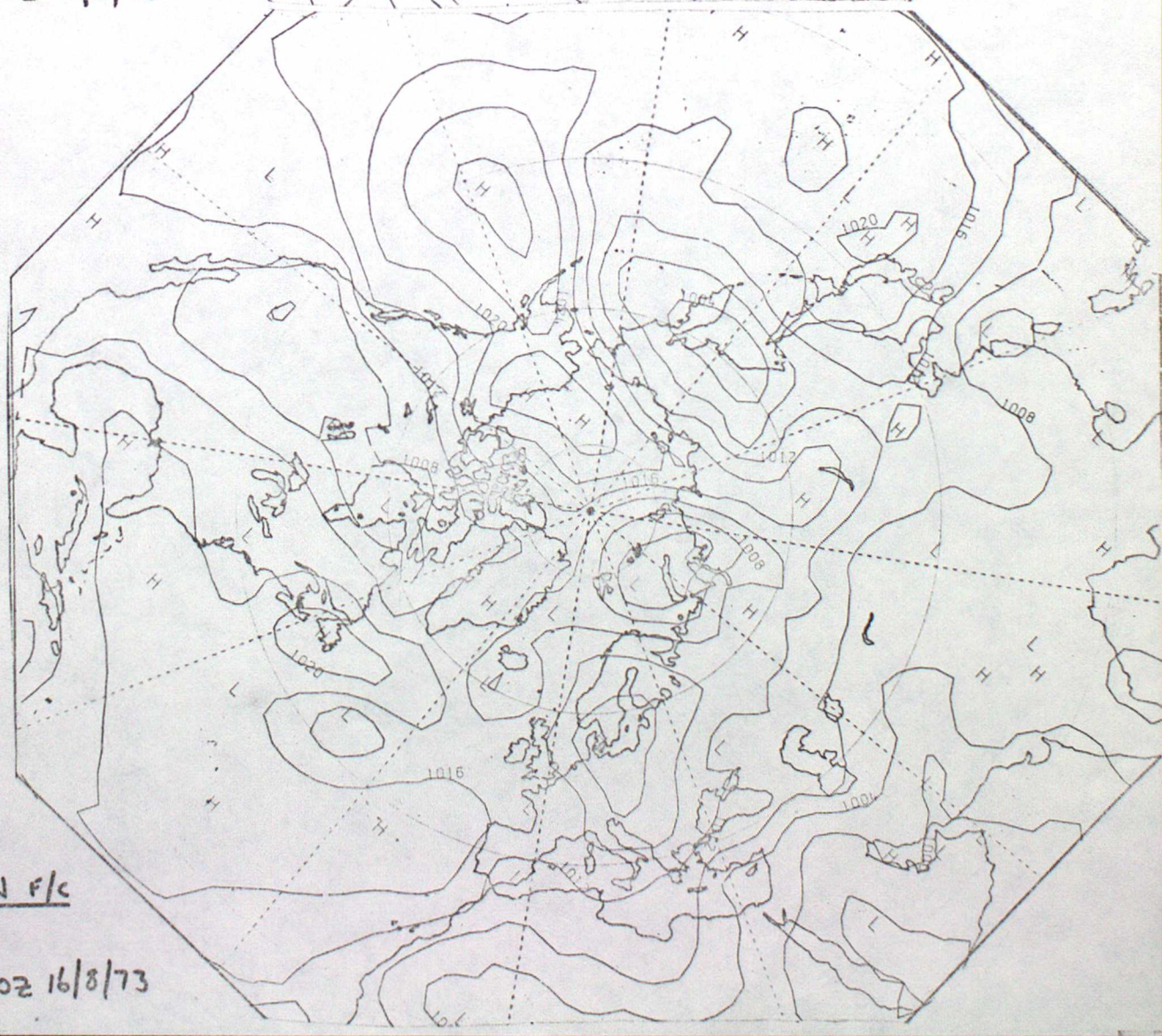

NEW

FORMULATION F/C

T + 24

VERIFYING: 00Z 16/8/73

FIG. 20

ANALYSIS

12Z 3/4/73

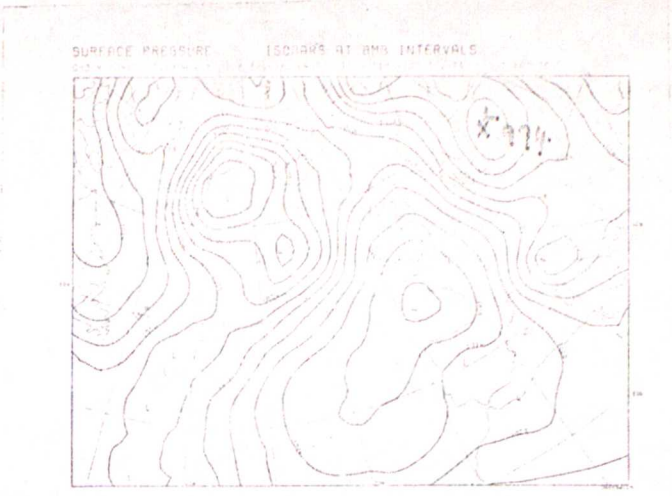

FIG. 21

OPERATIONAL F/C

T+36

VERIFYING: 12Z 3/4/73

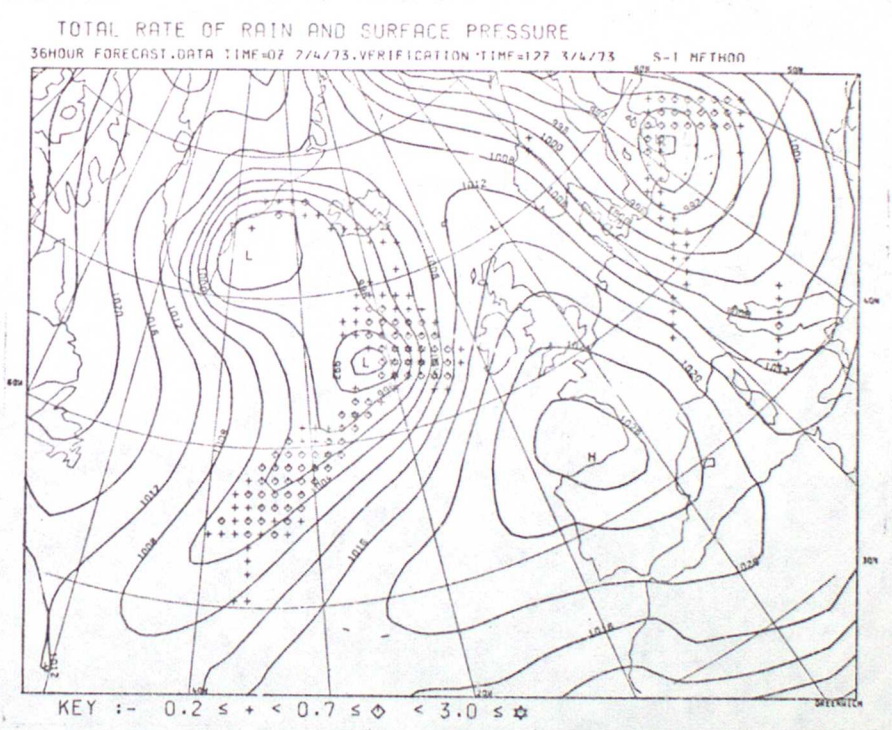

FIG. 22

NEW FORMULATION F/C

T+36

VERIFYING: 12Z 3/4/73

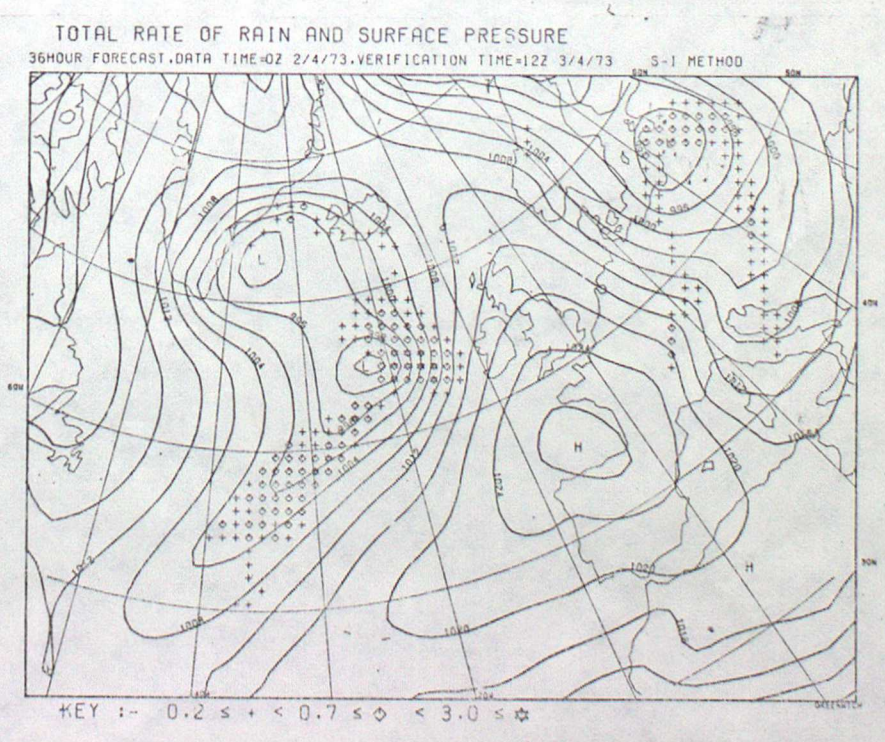

FIG. 23

ANALYSIS

00Z 6/4/73

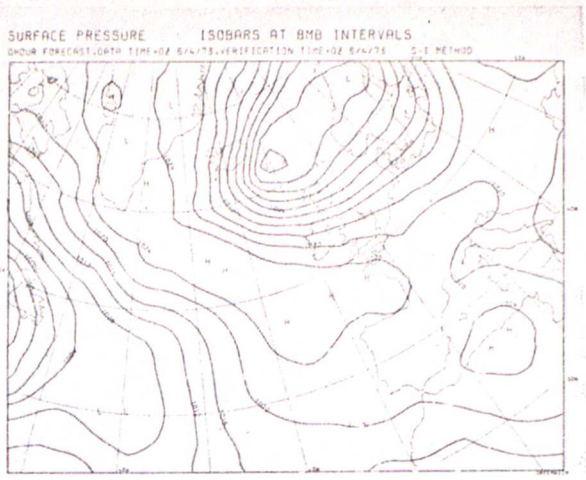

FIG. 24

OPERATIONAL F/C

T+36

VERIFYING: 00Z 6/4/73

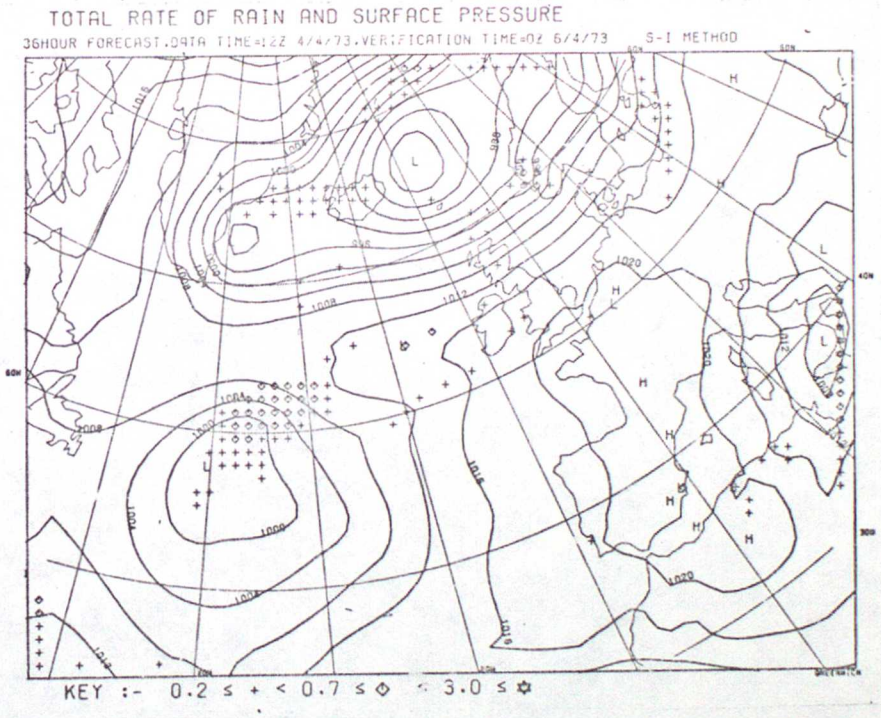

FIG. 25

NEW FORMULATION F/C

T+36

VERIFYING: 00Z 6/4/73

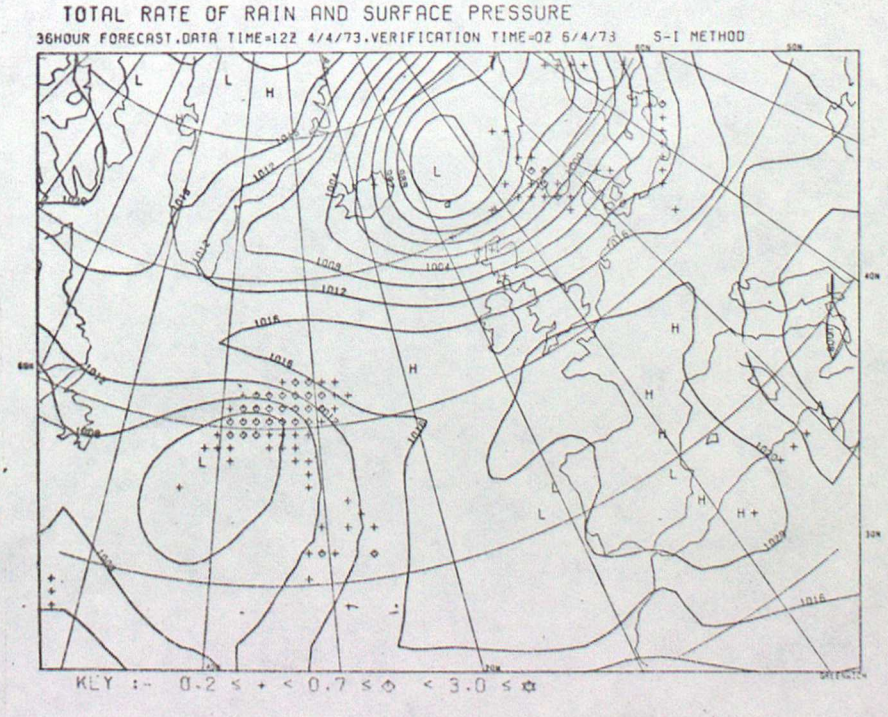

FIG. 26

ANALYSIS

12Z 30/11/73

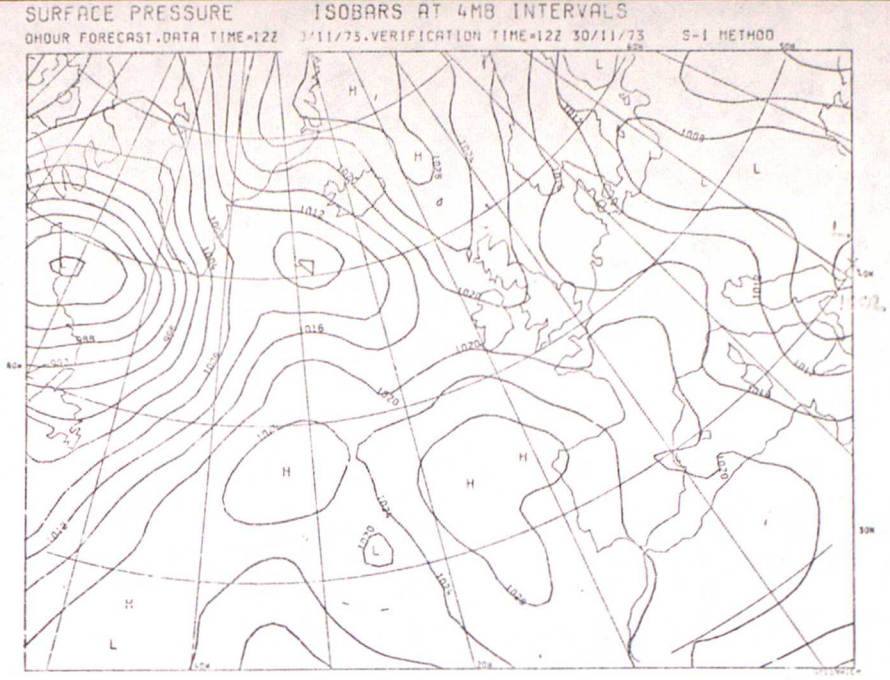

FIG. 27

OPERATIONAL F/C

T + 36

VERIFYING: 12Z 30/11/73

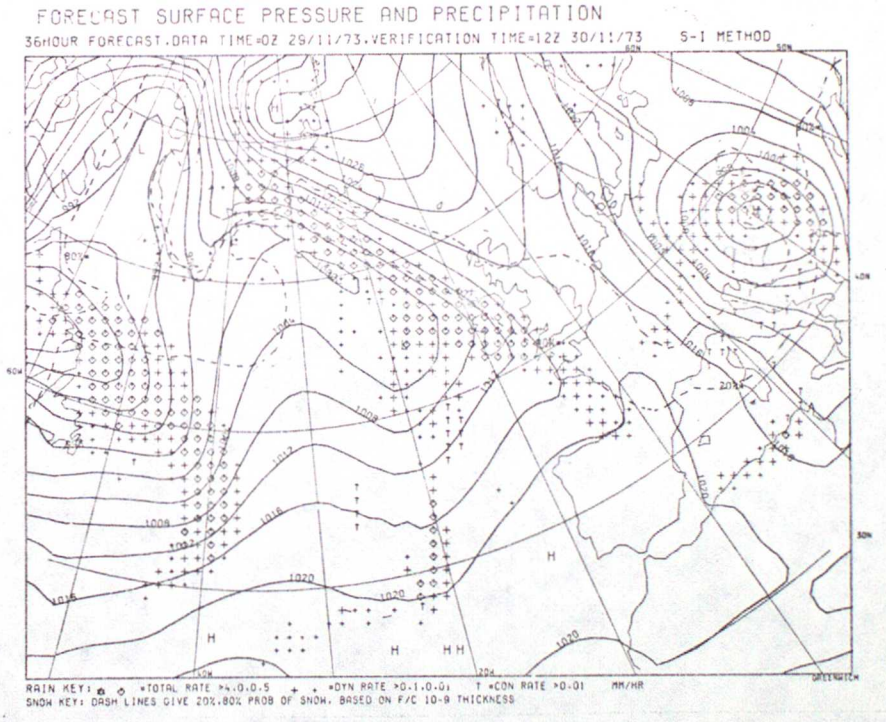

FIG. 28

NEW FORMULATION F/C

T + 36

VERIFYING: 12Z 30/11/73